Imaging from topography with Fourier methods

Gary F. Margrave and Zhengsheng Yao

ABSTRACT

The method of wavefield extrapolation by nonstationary phase shift is extended to the case of data recorded on a topographic surface. Using the NSPS (nonstationary phase shift) algorithm, the space-domain input data is phase shifted to a horizontal datum beneath the lowest topographic point. The nonstationary phase shift simultaneously accounts for lateral velocity variations and the lateral variation of downward step size. The f-k spectrum of the downward continued data is synthesized at the datum. A much more computationally expensive pseudo-inverse technique is also formulated for comparison. Tests on simple synthetics show that the NSPS method works nearly as well as the pseudo-inverse technique.

INTRODUCTION

Nonstationary phase shift methods have been developed at CREWES and elsewhere (Margrave and Ferguson, 1997 and 1999) to extrapolate wavefields through complex media. The key concept is to generalize the stationary phase shift method of Gazdag (1978) by allowing the velocity to depend upon the coordinates transverse to the direction of extrapolation. It was shown that this leads to a generalization of the PSPI (phase shift plus interpolation) method that has been independently derived by Fishman and McCoy (1985). A further method, called NSPS (nonstationary phase shift) was discovered and is now known to be the transpose (in lateral coordinates) of PSPI. Both of these forms are expressible as generalized Fourier integrals known as nonstationary filters or equivalently as pseudodifferential operators.

The essential feature of these new Fourier extrapolators is their ability to allow simultaneous dependence upon a space variable and its corresponding Fourier wavenumber. This generalizes the classical phase shift, that depends upon transverse wavenumber, to one that allows the velocity to depend upon the transverse coordinate. This same feature can accommodate topographic variations of the surface on which the seismic recording takes place by allowing an initial downward extrapolation step size that depends upon the lateral coordinate.

For simplicity, suppose a horizontal datum plane is defined slightly beneath the lowest topographic point and that a velocity model is available for the volume between the datum and the topography. Then, a downward extrapolation step, whose magnitude is the elevation difference between the topography and the datum at each lateral coordinate, can be accomplished with nonstationary filter theory. A further complication arises in that the recorded data cannot be regarded as being regularly sampled in space. Even if care is taken to accomplish regular sampling in the horizontal coordinate, the topographic variation means that the sampling is irregular in the vertical coordinate. This means that the f-k spectrum of data recorded on the

topography is not well estimated with fft methods that assume regular sampling. Consequently, the methods considered here assume the input data is in the space domain and estimate the f-k spectrum at the datum.

DERIVATION OF TOPOGRAPHIC EXTRAPOLATION

Consider the geometry shown in Figure 1 where the datum plane is taken at z=0 and the topography is given by z=-h(x) where h(x) is a positive function giving the topographic elevation above the datum. Then, an expression to upward continue upgoing acoustic waves from z=0 to z=-h(x) using the PSPI algorithm is

$$\psi\left(x,-h(x),\omega\right) = \frac{1}{2\pi}\int_{-\infty}^{\infty} \varphi\left(k_x,0,\omega\right)\alpha_-\left(k_x,x,\omega\right)\exp\left(ik_x x\right)dk_x \qquad (1)$$

where

$$\alpha_-\left(k_x,x,\omega\right) = \exp\left(-ih(x)\sqrt{\frac{\omega^2}{v(x)^2} - k_x^2}\right). \qquad (2)$$

In equation (1) $\varphi(k_x,0,\omega)$ is the spectrum of the data at the datum and the $-$ subscript on α indicates the direction of extrapolation. The insertion of the function h(x) in the extrapolation phase shift accomplishes a variable-size extrapolation step. In this way, we implicitly avoid the issue of the proper calculation of the f-k spectrum of the recorded data.

We explore two options to recover $\varphi(k_x,0,\omega)$ given $\psi(x,-h(x),\omega)$. First, we consider the approximate inverse to equation (1) using the NSPS extrapolator (Margrave and Ferguson, 1998). That is

$$\varphi_N\left(k_x,0,\omega\right) = \int_{-\infty}^{\infty} \psi\left(x,-h(x),\omega\right)\alpha\left(k_x,x,\omega\right)\exp\left(ik_x x\right)dx \qquad (3)$$

where $\alpha(k_x,x,\omega)$ is the complex conjugate of $\alpha_-(k_x,x,\omega)$. This expression has the advantages of simplicity and that it does not, in principle, require that $\psi(x,-h(x),\omega)$ be regularly sampled. This is analogous to computing the spectrum of an irregularly sampled function by direct implementation of the forward DFT (discrete Fourier transform). Letting L_N symbolize the integral operator of equation (3), we have

$$\varphi_N\left(k_x,0,\omega\right) = L_N\psi \approx \varphi\left(k_x,0,\omega\right). \qquad (4)$$

Here the middle form recreates equation (3) while the final form expresses the expectation that φ_N approximates φ. If L_{P-} is the linear integral operator of equation (1), then equation (4) expresses the fact that $L_N L_{P-} \sim 1$ (Margrave and Ferguson, 1998).

Second, we consider the generalized, or pseudo-inverse, to (1)

$$\varphi_g\left(k_x, 0, \omega\right) = L_g^{-1}\psi \ . \tag{5}$$

If the square matrix $L_P{}^T L_P$ is of full rank, then the generalized inverse is equivalent to a least-squares solution. This approach is known to be a better solution to the irregular data problem than the direct forward DFT (discrete Fourier transform) similar to equation (3). Equation (5) can be computed directly using any of a variety of numerical techniques. In this work we have used Matlab's pseudo-inverse function *pinv*.

Equation (4) can be viewed as an approximation to equation (5). Since $L_N L_{P_-} \sim 1$ we can infer that $L_N \sim L_P^{-1}$; however, L_g^{-1} will generally be a much stronger inverse for L_P.

EXAMPLES

As an illustration of these topics, Figure 2 shows a simple topographic profile while Figure 3 shows an input wavefield consisting of eight horizontally aligned impulses. In Figure 4 is the result of upward extrapolating these impulses to the topography, using the PSPI expression of equation (1) and a recursive sequence of 5 m steps. Since the PSPI algorithm becomes very accurate in the limit of small extrapolation steps, this can be considered as a nearly exact forward model. A constant velocity of 2000 m/s was assumed and close inspection of Figure 4 shows that the diffraction responses have identical asymptotic slopes but differing delays.

In Figure 5 is shown the result of using NSPS (equation (3)) to extrapolate the wavefield of Figure 4 back down to the starting elevation. Unlike the upward extrapolation, this was done in a single step whose magnitude varies with lateral position. The resulting focal points are quite good for a test of this sort. Perfect impulses are not recovered because inverse wavefield extrapolation never attempts to recover the evanescent portion of the wavefield. Inversion of the evanescent frequencies requires the application of a growing real exponential which is unstable. The best that can be achieved is the recovery of an "x" pattern at each impulse position. This result has achieved the expected image except that there is some slight spatial variation in quality.

A full inversion using the pseudo-inverse calculation is shown in Figure 6. Remarkably, this has recovered an almost-perfect image of the input wavefield. This is because, in a noise-free simulation with high precision numerics, the pseudo-inverse approach actually inverts the evanescent energy. It is interesting that, even though the forward wavefield was calculated with 15 extrapolation steps, the inverse was accomplished by inverting a one-step model. The full inversion of equation (5) required $\sim 10^{11}$ floating point operations while the direct NSPS approach of Figure 4 required only $\sim 10^8$ floating point operations.

A more realistic example uses the input dataset of Figure 7 that is identical to that of Figure 3 but with 5% random noise added. The single-step NSPS inverse

extrapolation is shown in Figure 8 and comparison with Figure 5 shows that the result is just as good as before.

If the noisy data is inverted as before with the pseudo-inverse approach, the result is unusable due to a tremendous amplification of the noise caused by attempted inversion of the evanescent energy. Instead, a pseudo-inverse was used in which singular values smaller that 4% of the maximum are not inverted. The result, shown in Figure 9 is quite different from the exact result of Figure 6 and actually is similar to that obtained, with much less effort, using NSPS (Figure 5). The width of the focal points is determined by the back propagation of non-evanescent energy and is similar in both Figures 9 and 5.

The strong diagonal artifacts seen in the inversion of Figure 9 can be reduced by inverting yet fewer singular values (a softer inversion) as shown in Figure 10. In this case singular values less than 12% of the maximum were not inverted. Though the inversion quality is improved, the process still takes much longer than the one-step NSPS result.

A final example of a more extreme topography problem is shown in Figure 11. Here the topographic variation is nearly three times that of the previous model and the velocity field between topography and datum (at 0 meters) shows complex variation. The forward-modeled response (using the same input wavefield (Figure 2)) is shown in Figure 12 and its f-k spectrum is in Figure 13. The f-k spectrum of the data in Figure 2 is shown in Figure 14 for comparison with Figure 13. The complex (x,t) domain recording at the topography can be seen to have a muddied f-k spectrum instead of the clear spectral lines of the input. (A constant-velocity phase shift from one horizontal datum to another preserves these lines.)

The result of a single NSPS downward step is shown in Figure 15 and its f-k spectrum is in Figure 16. A very good focus of each image point has been achieved and the f-k spectral lines have been resolved fairly well. The variable velocity structure beneath the topography suggests that better results could be obtained in this case by recursively stepping to the datum. Figures 17 and 18 show the wavefield and spectrum after taking five recursive steps to datum using the NSPS algorithm. In comparison with the single-step results (Figures 15 and 16) the focal points are sharper and the spectral lines are better resolved. In this case, more steps are not much better as is seen in Figures 19 and 20 where twenty recursive steps were taken.

The recursive stepping was implemented by dividing the distance from the topographic maximum to datum into n equal intervals. Across each interval, a variable-size extrapolation step is taken. The step magnitude is zero if the topography is beneath the bottom of the interval, equal to the interval thickness if the topography is above the top of the interval, and equal to the distance from the topography to the bottom of the interval for the intermediate case.

From the perspective of resolution, it is noteworthy that the impulses beneath the topographic highs (e.g. the fourth and sixth from the left) are better resolved than

those beneath lower spots. This is probably because the anticline topography allows a wider range of scattering angles to be captured.

DISCUSSION

There are many other methods for migration from topography. One of the simplest is to simply perform a Kirchhoff migration that raytraces traveltimes directly from the topographic surface as in Wiggins (1984). An alternative approach has been the use of the "zero-velocity layer" (Beasley and Lynn, 1992; Gray, 1997) in conjunction with recursive finite-difference algorithms. This latter assumes that data have been static-shifted to a horizontal datum above the highest point of the topography. Wave-equation downward continuation is done assuming zero velocity (for diffraction effects only) between the datum and the topography.

The method proposed here is most closely related to the zero-velocity layer, in that a recursive downward continuation is done, but is distinct from it in that the downward step size is modified, not the velocity. Conceptually, we advocate stepping downward directly from the topography to a horizontal datum (below the lowest topographic point) using a step size that is the vertical distance from the topography to datum. For strong velocity variations, we advocate a similar process using a series of recursive steps. This method does not require separating diffraction and thin-lens effects in the extrapolator and is in approximate accord with the wave equation. Furthermore, since we use the NSPS extrapolator, that expects a space domain input, we do not assume that the data is regularly sampled on the acquisition surface.

Many other problems remain to be assessed and addressed to make this a practical algorithm. For example, geometric irregularities other that those due to topographic fluctuations will cause additional difficulties in computing accurately the integral in equation (3). Also, statics solutions are still the most reliable method of estimating in short-wavelength variations in the near surface. A practical implementation of our method must define how statics solutions should be incorporated. This is especially problematic with residual statics techniques because they only estimate traveltime delays and do not produce a near surface model.

More realistic topographic models should also be studied. The occurrence of great topographic relief is often associate with thrust faulting and that can lead to strong velocity gradients in the near surface that are much different than those modelled in this study.

CONCLUSIONS

We have demonstrated that nonstationary phase shift methods, particularly NSPS, can accurately account for topographic effects. The method advocated uses a nonstationary phase shift that incorporates a laterally variable extrapolation step size in addition to laterally variable velocity. Synthetic tests show results with NSPS that are similar to a much more computationally expensive pseudo-inverse approach.

ACKNOWLEDGMENTS

REFERENCES

Beasley, C., and Lynn, W., 1992, The zero-velocity layer: migration from irregular surfaces: Geophysics, **57**, 1435-1443.
Fishman, L., and McCoy, J.J., 1985, A new class of propagation models based on a factorization of the Helmholtz equation: Geophys. J. R. astr. Soc., **80**, 439-461.
Gazdag, J., 1978, Wave equation migration with the phase-shift method: Geophysics, **43**, 1342-1352.
Gazdag, J., and Squazzero, P., Migration of seismic data by phase shift plus interpolation: Geophysics, **49**, 124-131.
Gray, S. H., 1997, Where is the zero-velocity layer: Geophysics, **62**, 266-269.
Margrave, G.F., and Ferguson, R.J., 1997, Wavefield extrapolation by nonstationary phase shift: 67th Annual SEG meeting, Dallas, Texas.
Margrave, G.F. and Ferguson, R.J., 1999, Wavefield extrapolation by nonstationary phase shift: Geophysics, **64**, 1067-1078.
Margrave, G.F., and Ferguson, R.J., 1998, Nonstationary filters, pseudodifferential operators, and their inverses: CREWES Annual Research Report, **10**, chapter 26.
Wiggins, J. W., 1984, Kirchhoff integral extrapolation and migration of nonplanar data: Geophysics, **49**, 1239-1248.
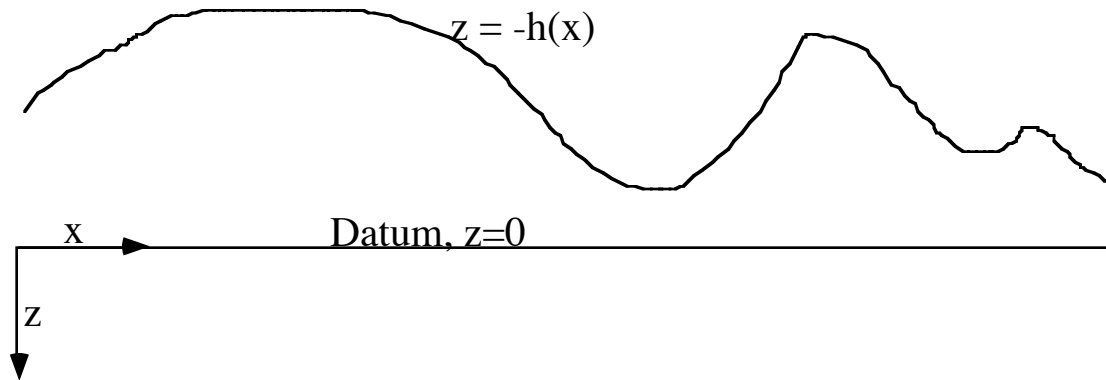
Figure 1. The coordinate system and datum plane used in the theoretical description.
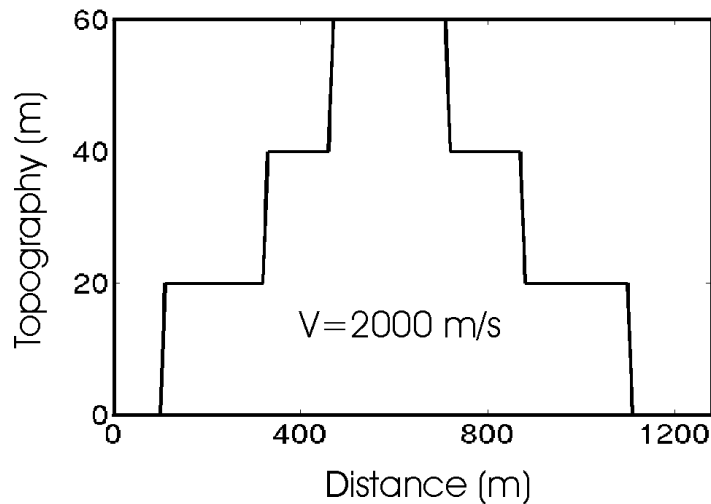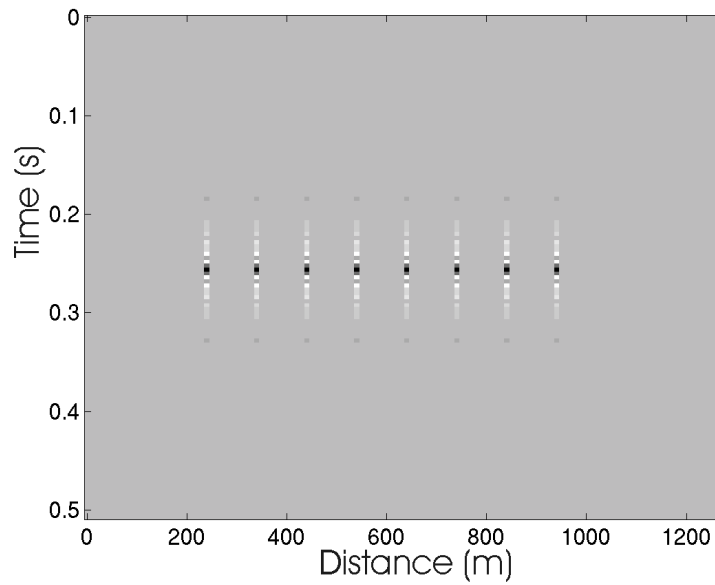

Figure 2. A simple topographic model.

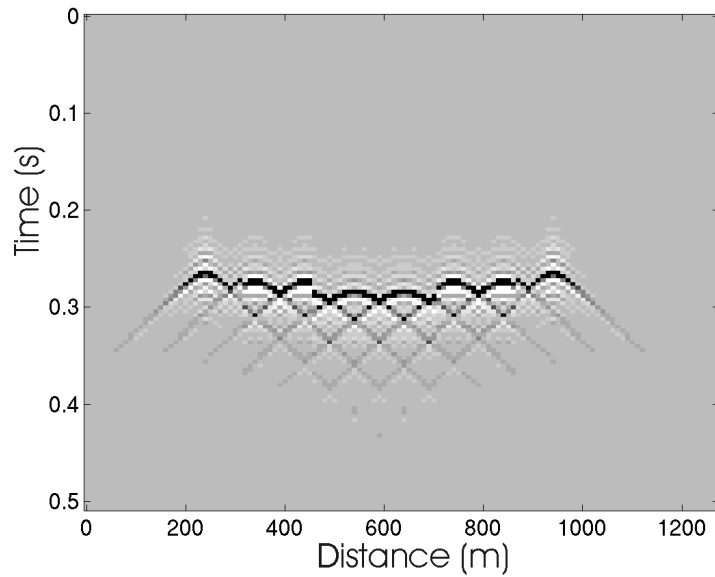Figure 3. The input wavefield into the synthetic studies.

Figure 4. The result of upward extrapolating the wavefield of Figure 3 from z=0 to the topographic curve of Figure 2. The PSPI algorithm was used with 5 m depth steps.
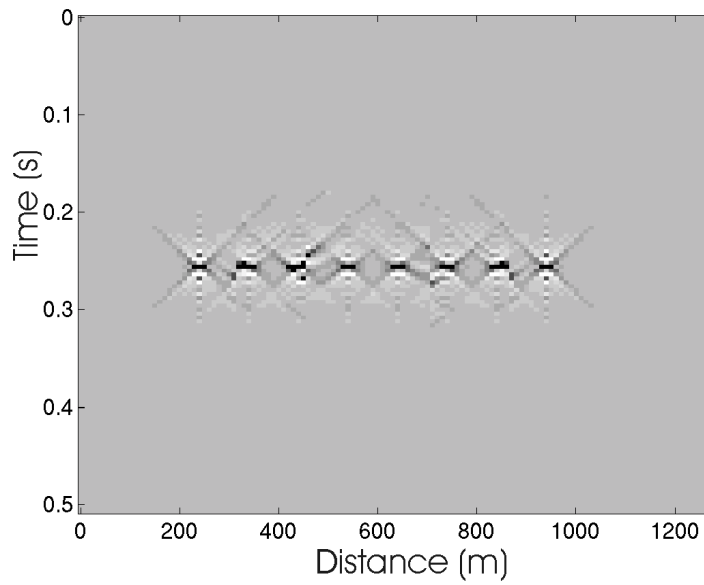
Figure 5. The result of downward continuing the wavefield of Figure 4 from the topography to the datum at z=0. The NSPS algorithm was used and a single laterally-variable extrapolation step was taken.
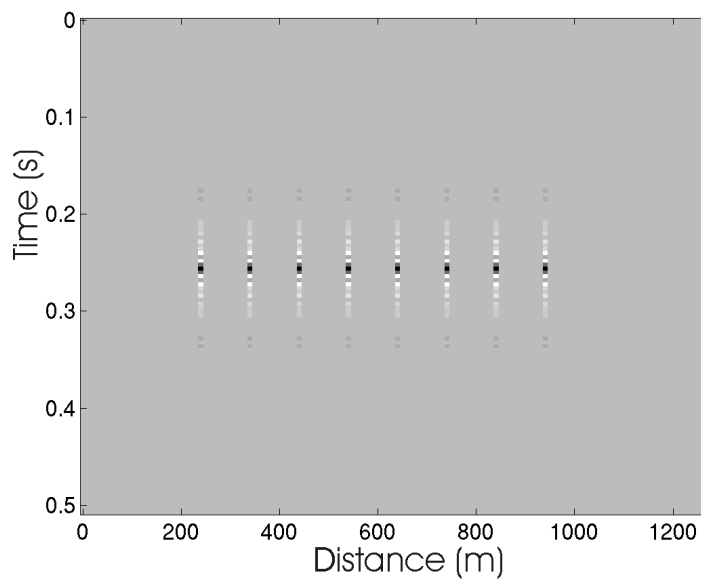

Figure 6. The result of pseudo-inverse downward continuation, from topography to datum, of the wavefield of Figure 4.
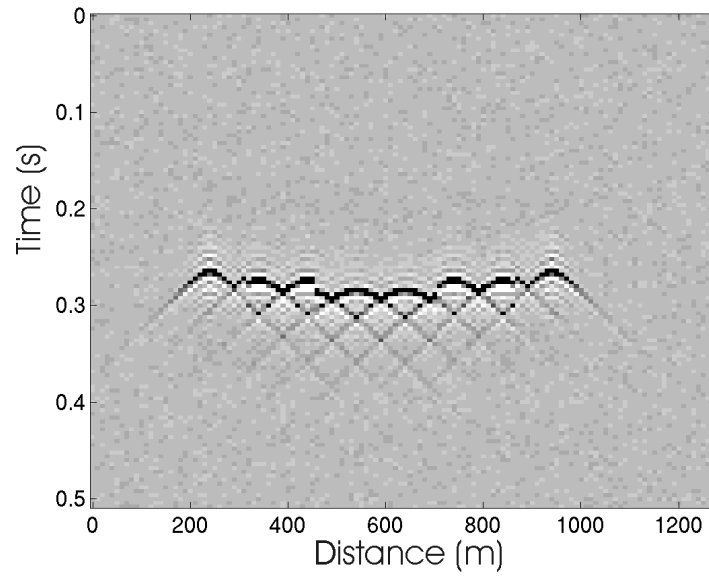
Figure 7. The wavefield of Figure 4 with a low-level of random noise added.
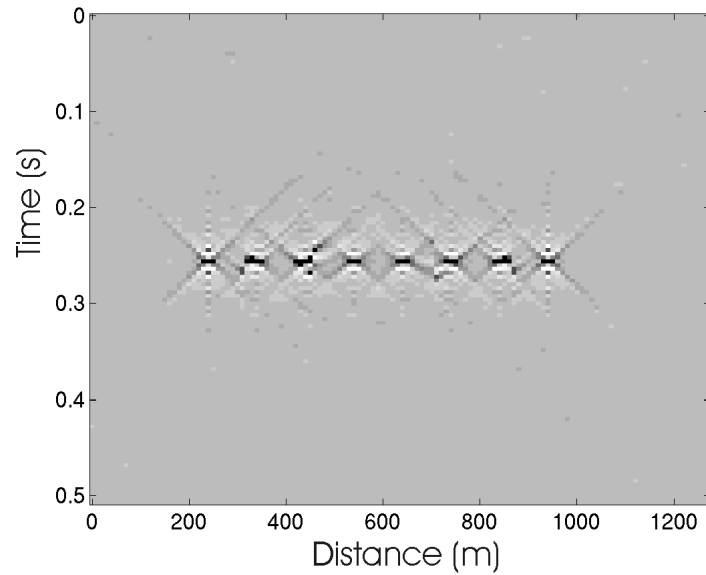

Figure 8. The result of downward extrapolation, from topography to datum, of the wavefield of Figure 7. A single step with the NSPS algorithm was used. Compare with Figure 5.
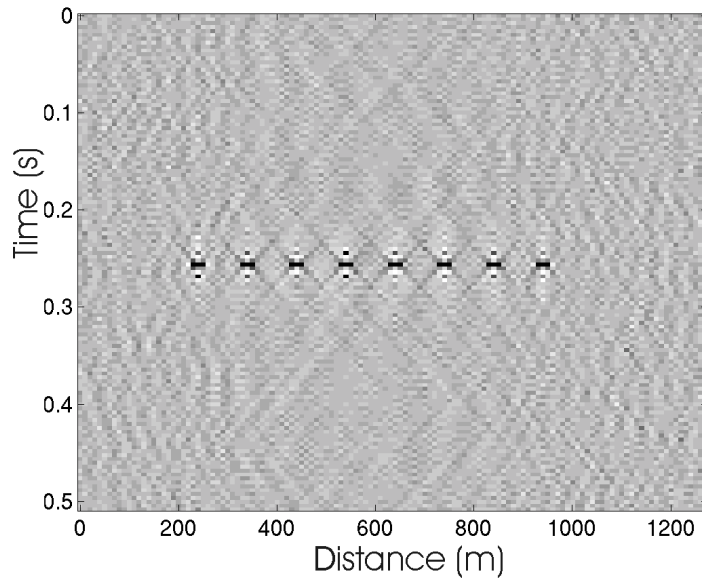
Figure 9. A pseudo-inverse downward continuation of the dataset of Figure 7. Most, but not all, singular values of L_P were inverted.
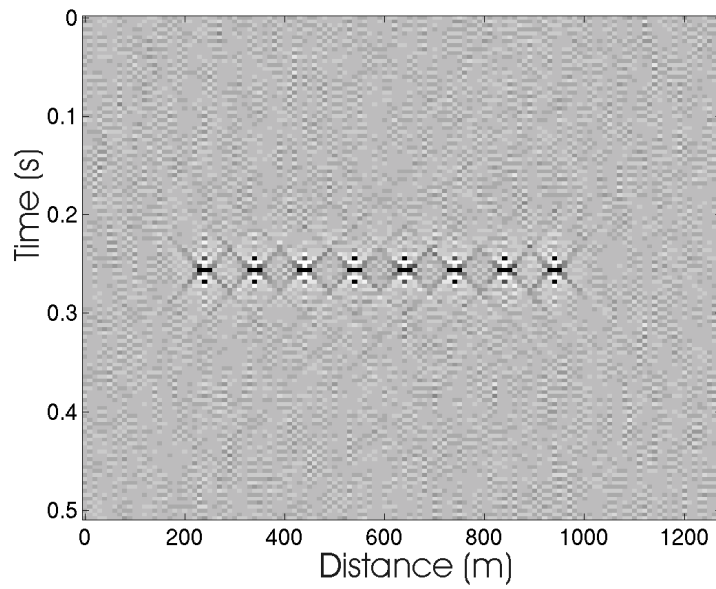

Figure 10. Similar to Figure 9 except that fewer singular values were inverted.